THE JOURNAL OF BIOLOGICAL CHEMISTRY VOL. 291, NO. 2, pp. 547–559, January 8, 2016
© 2016 by The American Society for Biochemistry and Molecular Biology, Inc. Published in the U.S.A.

Validation and Characterization of a Novel Peptide That Binds Monomeric and Aggregated β-Amyloid and Inhibits the Formation of Neurotoxic Oligomers*

Received for publication, July 21, 2015, and in revised form, October 28, 2015 Published, JBC Papers in Press, November 4, 2015, DOI 10.1074/jbc.M115.679993

Renae K. Barr[‡§1], **Giuseppe Verdile**[¶‖**1,2], **Linda K. Wijaya**[‡], **Michael Morici**[‡], **Kevin Taddei**[‡‖], **Veer B. Gupta**[‡§‖], **Steve Pedrini**[‡§‖], **Liang Jin**[‡‡], **Joseph A. Nicolazzo**[‡‡], **Erin Knock**[§§], **Paul E. Fraser**[§§], **and Ralph N. Martins**[‡§‖**3]

From the [‡]*Centre of Excellence for Alzheimer's Disease Research and Care School of Medical Sciences, Edith Cowan University, 270 Joondalup Dr., Joondalup, Western Australia 6027,* [§]*Alzhyme Pty Ltd., Nedlands, Western Australia 6009, the* [¶]*School of Biomedical Sciences, Faculty of Health Sciences, Curtin University, Bentley, Western Australia 6102, the* [‖]*Sir James McCusker Alzheimer's Disease Research Unit, Suite 22, Hollywood Medical Centre, 85 Monash Ave., Nedlands, Western Australia 6009, the* [**]*School of Psychiatry and Clinical Neurosciences, University of Western Australia, Crawley 6009, the* [‡‡]*Drug Delivery, Disposition and Dynamics, Monash Institute of Pharmaceutical Sciences, Monash University, 381 Royal Parade, Parkville, Victoria 3052, Australia, and the* [§§]*University of Toronto, Tanz Centre for Research in Neurodegenerative Diseases, Krembil Discovery Tower, 60 Leonard Ave., Toronto, Ontario M5T 2S8, Canada*

Although the formation of β-amyloid (Aβ) deposits in the brain is a hallmark of Alzheimer disease (AD), the soluble oligomers rather than the mature amyloid fibrils most likely contribute to Aβ toxicity and neurodegeneration. Thus, the discovery of agents targeting soluble Aβ oligomers is highly desirable for early diagnosis prior to the manifestation of a clinical AD phenotype and also more effective therapies. We have previously reported that a novel 15-amino acid peptide (15-mer), isolated via phage display screening, targeted Aβ and attenuated its neurotoxicity (Taddei, K., Laws, S. M., Verdile, G., Munns, S., D'Costa, K., Harvey, A. R., Martins, I. J., Hill, F., Levy, E., Shaw, J. E., and Martins, R. N. (2010) *Neurobiol. Aging* 31, 203–214). The aim of the current study was to generate and biochemically characterize analogues of this peptide with improved stability and therapeutic potential. We demonstrated that a stable analogue of the 15-amino acid peptide (15M S.A.) retained the activity and potency of the parent peptide and demonstrated improved proteolytic resistance *in vitro* (stable to $t = 300$ min, *c.f.* $t = 30$ min for the parent peptide). This candidate reduced the formation of soluble Aβ42 oligomers, with the concurrent generation of non-toxic, insoluble aggregates measuring up to 25–30 nm diameter as determined by atomic force microscopy. The 15M S.A. candidate directly interacted with oligomeric Aβ42, as shown by coimmunoprecipitation and surface plasmon resonance/Biacore analysis, with an affinity in the low micromolar range. Furthermore, this peptide bound fibrillar Aβ42 and also stained plaques *ex vivo* in brain tissue from AD model mice. Given its multifaceted ability to target monomeric and aggregated Aβ42 species, this candidate holds promise for novel preclinical AD imaging and therapeutic strategies.

Alzheimer disease (AD)[4] is a progressive neurodegenerative disorder, accounting for 50–70% of late-onset dementia cases (2). The major biochemical hallmarks of AD are extracellular amyloid plaques and intracellular neurofibrillary tangles. The predominant species present in amyloid plaques is β-amyloid (Aβ), a 4.5-kDa peptide generated through amyloidogenic processing (sequential cleavage by β- and γ-secretases) of the parent amyloid precursor protein (APP). This produces two forms of Aβ, comprising either 40 or 42 amino acids, where the relative amount of the longer 42-amino acid form (Aβ42) is especially critical for AD progression, given its higher propensity to aggregate and form neurotoxic species (3, 4).

In AD brain, the monomeric Aβ42 peptide is known to aggregate and form various ordered assemblies, which precede plaque formation. These include low-*n* oligomers (dimers to octamers, reviewed in Ref. 5), high molecular weight oligomers such as Aβ-derived diffusible ligands (6) and globulomers (7), protofibrils (8), and fibrils (9). Much evidence has indicated that soluble Aβ42 oligomers, rather than mature amyloid plaques, correlate with disease severity (10, 11) and contribute to synaptic degeneration and neurotoxicity (12, 13). In particular, recent work has highlighted a role for dimers, trimers, and dodecamer forms of Aβ oligomers in neuronal dysfunction (see Refs. 14 and 15 and reviewed in Ref. 5).

* This work was supported in part by the National Health and Medical Research Council of Australia Project Grant 595300 and Postdoctoral Fellowship 430909 (to R. K. B), Alzhyme Pty Ltd., and Edith Cowan University. R. N. M. is shareholder and CSO of Alzhyme Pty, LTD. No other conflicts of interest to declare.

[1] Both authors contributed equally to this work.

[2] Supported by Curtin University Research Fellowship CRF140196. To whom correspondence may be addressed: School of Biomedical Sciences, Faculty of Health Sciences, Curtin University, Bentley, WA, Australia. Tel.: 61-8-9266-5618; Fax: 61-8-9266-1715; E-mail: giuseppe.verdile@curtin.edu.au.

[3] To whom correspondence may be addressed. Centre of Excellence for Alzheimer's Disease Research and Care, Sir James McCusker Alzheimer's Disease Research Unit (M650), Suite 22, Hollywood Medical Centre, 85 Monash Ave., Nedlands 6009, Western Australia. Tel.: 61-8-9347-4201; Fax: 61-8-9347-4299; E-mail: r.martins@ecu.edu.au.

[4] The abbreviations used are: AD, Alzheimer's disease; Aβ, β-amyloid; 15M S.A., stable analogue of 15-mer parent peptide; APP, amyloid precursor protein; Aβ42, 42-amino acid β-amyloid; 15-mer, 15-mer candidate peptide; 9-mer, 9-mer candidate peptide; 9M S.A., stable analogue of 9-mer candidate peptide; CTL1, scrambled control based on 9-mer candidate peptide; CTL1 S.A., stable analogue of CTL1 peptide; CTL2 S.A., stable analogue of 9-mer APP fragment control peptide; TMR, tetramethyl rhodamine; ThT, thioflavin T; LDH, lactate dehydrogenase; AFM, atomic force microscopy; RU, resonance units; oAβ42, oligomeric Aβ42; BBB, blood-brain barrier; MTS, 3-(4,5-dimethylthiazol-2-yl)-5-(3-carboxymethoxyphenyl)-2-(4-sulfophenyl)-2*H*-tetrazolium; BisTris, 2-[bis(2-hydroxyethyl)amino]-2-(hydroxymethyl)propane-1,3-diol.

Downloaded from http://www.jbc.org/ at CURTIN UNIV OF TECHNOLOGY (CAUL) on June 12, 2016

The accumulation of Aβ is thought to occur early in the disease process. Studies in transgenic mice show that cognitive deficits are associated with small Aβ oligomeric assemblies (16, 17), which precede amyloid deposition and promote Tau phosphorylation and tangle formation (18, 19). Further evidence for a pivotal role for Aβ oligomers in the neurodegenerative process is provided by the development of transgenic mice expressing oligomers, which show synaptic degeneration, Tau phosphorylation, and neuronal loss in the absence of plaques (20). Although these findings suggest interventions targeting Aβ oligomers have the potential to halt disease progression, oligomers have proved to be difficult therapeutic targets. This is partly due to the complex inter-conversion between different Aβ42 assemblies and the fact that Aβ42 oligomers of different structure, stability, and concentration may all be neurotoxic (reviewed in Ref. 21).

We have previously reported a novel 15-amino acid peptide isolated by subtractive phage display screening, which bound the toxic human Aβ42 peptide, but not the related, non-toxic rat Aβ42 peptide. This peptide was shown to target Aβ42 and attenuate its neurotoxicity (1). In an effort to generate a novel, specific and stable candidate peptide capable of targeting Aβ42 oligomers, we have exploited the known ability of this peptide to target Aβ42 and aimed to increase its utility using two approaches: (i) reduced length for improved permeability across the blood-brain barrier and peptidomimetic design; and (ii) increased proteolytic resistance. The stability of these analogues was assessed *in vitro* and their Aβ42 binding and activity was assessed biochemically. We have further provided proof-of-principle experiments to demonstrate that the lead candidate peptide shows potential as a preclinical AD imaging agent, given its ability to bind Aβ42 oligomers *in vitro*, amyloid plaques *ex vivo*, and its potential for transport across the blood-brain barrier *in vivo*.

Experimental Procedures

Peptides—Human synthetic Aβ42 peptide was purchased from the W.M. Keck Foundation Biotechnology Resource Laboratory (Yale University, New Haven, CT). All other unlabeled peptides used in this study (15-amino acid peptide (15-mer); (Ac-TNPNRRNRTPQMLKR-NH_2 = "L-ANA-1" (1)), 15M S.A. (stable retro-inverso analogue of 15-amino acid peptide; Ac-rklmqptrnrrnpnt-NH_2),[5] 9 amino acid peptide (9-mer) (15-mer fragment based on *in silico* modeling; Ac-NRTPQMLKR-NH_2 = L-ANA5),[5] 9M S.A (stable analogue of the 9-mer; Ac-rklmqptrn-NH_2),[5] CTL1 (scrambled control based on 9-mer, Ac-RNPKMQRTL-NH_2), CTL1 S.A. (stable analogue of CTL1, Ac-ltrqmkpnr-NH_2), CTL2 S.A. (retro-inverso stable analogue control based on unrelated APP 9-amino acid peptide fragment as reported in Ref. 1; Ac-tlGsGprtt-NH_2) were obtained from Mimotopes, (Melbourne, Australia). Tetramethyl rhodamine (TMR)-labeled 15M S.A. and CTL2 S.A. were also obtained from Mimotopes (Melbourne, Australia). Tritium labeling of 15M S.A. peptide was performed by American Radiolabeled Chemicals, Inc. (St. Louis, MO).

Preparation of Aβ42 Monomers, Oligomers, and Fibrils—Aβ42 assemblies were prepared as preciously described (22). Briefly, Aβ42 was solubilized in 1,1,1,3,3,3-hexafluoro-2-propanol (Sigma), dried, and reconstituted in dry dimethyl sulfoxide (Sigma) to 5 mM concentration. For monomeric Aβ42, the 5 mM stock was diluted to 100 μM in ice-cold Milli-Q water and used immediately. For oligomeric and fibrillar Aβ42, the 5 mM stock was diluted to 100 μM in either ice-cold Ham's F-12 media (C-72110, PromoCell GmbH, Germany) or 10 mM HCl, respectively, and incubated for 24 h at either 4 or 37 °C, respectively.

In Vitro Assay of Peptide Stability—Peptides were prepared as either 1 or 4 mM solution in PBS. 20 μl of the peptide solution was diluted in either 10% rat brain homogenate (in PBS + 0.5% Triton X-100) or 100% serum. The solution was incubated at 37 °C for different times, and the reaction was stopped by adding cOmplete protease inhibitor mixture (Roche Molecular Biochemicals, Mannheim, Germany). For 9-mer and 9M S.A., the bulk of the brain proteins (but not the peptides) were precipitated in cold methanol (1:4 (v/v) mixture/methanol) for 1 h at −20 °C. The precipitated proteins were pelleted by centrifugation (10,000 × *g*, 10 min, 4 °C). The supernatant containing the peptide was concentrated five times under vacuum and separated by reversed-phase HPLC (RP-HPLC). Due to recovery issues with the longer 15-mer and 15M S.A. peptides, samples were instead lyophilized, extracted in TFA, centrifuged to remove insoluble material, and separated by RP-HPLC. The area of the peak (UV absorbance at 205 nm) corresponding to the intact peptide was measured and compared with an equivalent sample incubated in PBS.

Thioflavin T Assays—This method was adapted from Ref. 23. Briefly, Aβ42 oligomers were centrifuged (18,000 × *g*, 4 °C, 1 min) to pellet insoluble material. The clarified supernatant (4.5 μg/10 μl of 100 μM stock) was added to a black-walled, clear bottom 96-well microplate (PerkinElmer Life Sciences) in triplicate. 200 μl of thioflavin T (ThT) (5 μM in 50 mM glycine NaOH, pH 8.5, 0.22 μM filtered) was added and the plates were read at 3–5 min post-addition in a FLUOSTAR OPTIMA instrument (excitation filter: 450 nm; emission filter: 490 nm; 30 s mix before reading; gain-adjust to highest reading). Samples were assayed in triplicate and the blank ThT fluorescence was subtracted from all readings. Candidate peptides were also assayed in the absence of Aβ42 for interference in the assay.

Cell Culture, Treatment, and Neurotoxicity Assay—M17 neuroblastoma cells were cultured similar to Ref. 1. Briefly, M17 cells were seeded in a 48-well plate (25,000 cells/well in 500 μl of 1:1 DMEM/Nutrient Mixture F12 (DMEM/F-12) (Life Technologies) + 10% fetal calf serum) overnight. 100 μM Aβ42 oligomer stocks (± candidate peptides) were diluted to 20 μM concentration in treatment medium (20% (v/v) Ham's F-12, 80% (v/v) DMEM (no phenol red)) and used to treat cells (50–60% confluence) for 4 days (37 °C, 5% CO_2). On the fourth day, the evaluation of neurotoxicity was performed by measuring release of lactate dehydrogenase (LDH) (CytoTox-ONE™ Homogeneous Membrane Integrity Assay, Promega) and cell viability (CellTiter96® Aqueous One Solution Cell Proliferation Assay (MTS), Promega), according to the manufacturer's recommendations. Samples were assayed in triplicate.

[5] IP Australia provisional patent application number 2013904077.

Downloaded from http://www.jbc.org/ at CURTIN UNIV OF TECHNOLOGY (CAUL) on June 12, 2016

SDS-PAGE and Western Immunoblotting—Samples for gel analysis were prepared in two ways, *i.e.* denaturing and nondenaturing conditions. Non-denatured samples were separated by electrophoresis using a modified Blue Native-PAGE protocol, as described in Ref. 24. Samples were diluted in MOPS loading buffer (50 mM MOPS, 50 mM Tris, 20% glycerol, 0.05% Coomassie, pH 7.7) without reducing agent and were not heat denatured prior to PAGE separation. Where insoluble material was present in the samples, denaturing conditions were employed to solubilize this material. In the denaturing conditions, samples were diluted in LDS sample buffer plus reducing agent (NuPAGE®), and heat denatured (72 °C, 10 min) prior to separation of proteins by SDS-PAGE using NuPAGE® Novex 4–12% BisTris gradient gels and MES SDS running buffer (Life Technologies). Samples were transferred onto either nitrocellulose (denatured samples) or PVDF (non-denatured samples) membranes using the iBlot® blotting system (Life Technologies). Samples were subjected to Western immunoblotting with WO2 antibody (25) (kindly provided by Prof. Colin Masters, University of Melbourne, Australia), to detect Aβ species. Bands were visualized using enhanced chemiluminescence (Amersham Biosciences ECL) and exposure to Hyperfilm ECL films (GE Healthcare). Films were scanned on a Bio-Rad GS-800 densitometer and densitometry was conducted with Bio-Rad Quantity One software.

Atomic Force Microscopy (AFM)—Samples for AFM were prepared and analyzed according to Ref. 22. Briefly, Aβ samples were spotted on freshly cleaved grade V1 muscovite mica and incubated for 5 min. Samples were then rinsed with 0.22-μm syringe-filtered double-distilled water and blow dried with several gentle pulses of compressed air (N_2). Samples were then visualized under the AFM (NT-MDT) using semi-contact mode with the following parameters: a minimum contact force, amplitude between 0.5 and 2 V (depending on the cantilever) to generate magnitude ~20 nA, and scan rates ~0.5–1 Hz. All data were processed using Nova NT-MDT Software version 1.1.0.1780.

Surface Plasmon Resonance/Biacore Assays—These experiments were performed using a Biacore 3000 Instrument (GE Healthcare) with a protocol modified from Ref. 26. Either 15M S.A. peptide, or Aβ42 monomer/aggregates, were immobilized on separate CM5 sensorchips (GE Healthcare). The 15M S.A. peptide was immobilized on a CM5 sensorchip via amine coupling, according to the manufacturer's instructions, to a level of 245 resonance units (RU) (1 RU = 1 pg of protein/mm^2). Monomeric, oligomeric, and fibrillar Aβ42 preparations were immobilized on another CM5 sensorchip (10 μM in 10 mM sodium acetate buffer (pH 4.0), injection for 5 min at a flow rate of 30 μl/min) to final levels of 9,084, 11,467, and 4,924 RU, respectively. Note that the oligomeric Aβ42 and fibrillar Aβ42 preparations were prepared 24 h prior to immobilization, whereas the monomeric Aβ42 was prepared immediately prior to immobilization to minimize its aggregation. For both sensorchips, a reference surface was prepared in parallel (with no addition of peptide), and used for subtraction of nonspecific binding. Sensorgrams were obtained using standard conditions of 30 μl/min flow rate and HBS-EP running buffer (0.01 M HEPES, pH 7.4, 0.15 M NaCl, 3 mM EDTA, 0.005% (v/v) surfactant P20 (GE Healthcare)) as outlined under "Results."

Coimmunoprecipitation Analysis—Alexa 488-labeled oAβ42 was prepared as described in Ref. 27 and incubated with TMR-labeled 15M S.A. peptide in 300-μl reactions in TBS + 0.05% Tween 20 (TBST) with gentle rotation for 16 h at 4 °C. Complexes were captured using 1 μg of 6E10 antibody (Covance) for Aβ (2 h, 4 °C) and then γ-bind-Sepharose/Protein G-Mag-Sepharose (GE Healthcare) (2 h, 4 °C). Following removal of the supernatant, the beads were washed (3 × 500 μl of TBST) and samples were separated by denaturing SDS-PAGE on 4–12% BisTris NuPAGE gels (Life Technologies). Fluorescently labeled peptides were visualized by in gel fluorescence using a Typhoon FLA 9500 imaging system (GE Healthcare).

Immunohistochemistry—Brains were obtained from 8-month-old 5xFAD or TgCRND8 AD model mice (28) or age-matched non-transgenic controls and post-fixed and embedded in the freezing medium as described in Ref. 29. Serial sagittal cryosections were cut at a thickness of 10 μm. Positive control staining for amyloid plaques was performed using thioflavin S (Thio S) as described in Ref. 30. After the removal of the freezing medium by serial changes of TBS (pH 7.4), the slide was incubated for 1 h at room temperature in blocking buffer (10% goat serum in TBS). The slides were then stained with 1 μM TMR-labeled 15M S.A. peptide in 2% goat serum/PBS for 2 h at room temperature. Excess unbound peptide was removed prior to mounting by extensive washing with TBS. The coverslip was mounted using Prolong Gold mounting media (Life Technologies).

Brain Uptake of ^{3}H-Labeled 15M S.A. following Intravenous Administration—Animal experiments were approved by the Monash Institute of Pharmaceutical Sciences Animal Ethics Committee and were performed in accordance with the Australian National Health and Medical Research Council (NHMRC) guidelines for the care and use of animals for scientific purposes. Male Swiss Outbred mice (6–8 weeks of age; 25–30 g) were used in the studies and had free access to food and water during the experimental periods. An aliquot (50 μl) containing 10 μCi of ^{3}H-labeled 15M S.A. peptide was administered to mice by tail vein (intravenous) injection. Brain and plasma samples were collected over a 0.5–4-h period and the concentration of 15M S.A. peptide in plasma and brain homogenate was performed by liquid scintillation counting (Tri-Carb 2800 TR; PerkinElmer Life Sciences). The brain concentrations were corrected by subtracting the brain microvascular volume (0.035 ml/g) using [^{14}C]sucrose as a vascular marker (31). As described previously (32), the brain to plasma ratio of ^{3}H-labeled 15M S.A. peptide was determined using the following formula: (corrected number of disintegrations per minute (dpm) per g of brain tissue)/(number of dpm per ml of plasma). The intactness of ^{3}H-15M S.A. at post-dose time points following intravenous administration was assessed by HPLC. Briefly, brain samples were homogenized in a volume of MilliQ water (in ml) equal to twice the weight (in g) of the tissue using a glass rod. To 300 μl of brain homogenate or 100 μl of plasma, the same volume of acetonitrile was added prior to centrifugation at 14,100 × *g* for 5 min. An aliquot (100 μl) of the supernatant was then loaded onto a Waters Symmetry C_{18} column (5 × 4.6

Downloaded from http://www.jbc.org/ at CURTIN UNIV OF TECHNOLOGY (CAUL) on June 12, 2016

TABLE 1

Stability in 10% brain homogenate and 100% serum

9M S.A. and 15M S.A. show superior resistance to proteolytic degradation. Peptides were prepared as 1 or 4 mM solutions in PBS and diluted in 10% rat brain homogenate or 100% serum, respectively. Solutions were incubated at 37 °C for different times, and the reactions were stopped by addition of protease inhibitors. Samples were processed as described under "Experimental Procedures," separated by RP-HPLC and the level of intact peptide was determined at each time point.

Time (min)	Stability in 10% brain homogenate				Stability in 100% serum			
	15-mer	15M S.A.	9-mer	9M S.A.	15-mer	15M S.A.	9-mer	9M S.A.
min		*μg*				*μg*		
0	25.78	29.80	12.00	14.11	32.66	27.75	20.93	18.04
15	5.55	27.80	0.47	12.35	31.05	30.35	22.61	19.40
30	0.03	29.40	0	12.35	27.51	30.12	15.03	18.42
300	0.02	33.50	0	12.51	24.00	29.21	3.56	17.74

mm). Mobile phase A consisted of 0.1% (v/v) TFA in MilliQ water and mobile phase B consisted of 60% (v/v) acetonitrile in 0.1% (v/v) TFA in MilliQ water. ^{3}H-15M S.A. peptide was analyzed using the following gradient profile: 0 min, 95% A; 0–10 min, 70% A; 10–12 min, 95% A. The eluant from the column was collected every 0.5 min and the dpm of each fraction was measured by liquid scintillation counting. The profiles (dpm *versus* time) of brain and plasma samples were then generated and compared with those of ^{3}H-15M S.A. peptide solution as control.

Results

In Vitro Stability of Analogue Peptides with Increased Therapeutic Potential—To increase the membrane permeability and potential for peptidomimetic mimicry, we used *in silico* modeling to reduce the size of the parent 15-mer to a 9-mer. In addition, we employed modifications to both the parent 15-mer and the 9-mer to increase their resistance to proteolytic degradation, generating candidates denoted as 15M S.A. and 9M S.A.,[5] respectively. The *in vitro* stability of these peptides was measured following incubation in dilute rat brain homogenate or serum and HPLC quantification. For brain homogenate, we found that trace amounts of unmodified 15-mer and none of the unmodified 9-mer were present at $t = 30$ min (Table 1). In contrast, the concentrations of both stable analogue peptides remained relatively unchanged following an extended incubation of 300 min (Table 1). Similar findings were observed in 100% serum, where compared with unmodified peptide concentrations the stable analogues remained relatively unchanged across the incubation time points (Table 1). These results indicate that modifications to the 9-mer and 15-mer peptides reduced degradation and thus improved stability. These stable analogues were investigated further to determine whether they retained the activity of the parent peptides.

Effects on Aβ42 Aggregation and Neurotoxicity—Given the neurotoxicity attributed to oligomeric Aβ42, we next assessed the ability of the stable analogues to influence their formation and toxicity. We incubated monomeric Aβ42 peptide under conditions specifically favoring oligomerization for 24 h (22), in the presence or absence of the candidate peptides. We then assayed the Aβ42 aggregation in these samples using ThT fluorescence assays and Blue Native-PAGE/Western blotting. We additionally diluted samples to 20 μM Aβ42 concentration, treated M17 neuroblastoma cells, and quantified neurotoxicity following 4 days of treatment. ThT analysis revealed that both the parent 15-mer and 15M S.A. peptide reduced ThT fluorescence (and thus Aβ42 aggregation and oligomerization) in a dose-dependent manner and with similar potency (Fig. 1*A*). In comparison, the 9-mer peptide showed similar activity, but reduced potency, and the 9M S.A. peptide showed overlapping activity with a scrambled control peptide (CTL1) (Fig. 1*A*). Similar findings were observed when samples were analyzed by Blue Native-PAGE and Western blotting (Fig. 1*B*), where the presence of 15-mer and 15M S.A. resulted in a reduction in the Aβ42 aggregation "smear" evident at the 1:5 and 1:10 ratios of Aβ to peptide. The LDH assay indicated that a reduction in Aβ42 aggregation correlated with reduced neurotoxicity, with the parent 15-mer and 15M S.A. reducing neurotoxicity in a dose-dependent manner and with similar potency (Fig. 1*C*). In contrast, the 9-mer offered less potent neuroprotection and the activity of the 9M S.A. peptide was again similar to the scrambled control peptide (Fig. 1*C*). The neuroprotection offered by the candidate peptides was also confirmed using MTS assays, which indicated increases in cell viability in line with the reduction in toxicity evident in the LDH assays.[6] Together these findings indicated that the 15M S.A. candidate most effectively mimicked the activity and potency of the parent 15-mer peptide. Thus, this stable analogue was further characterized to provide insight into how it attenuates Aβ42-induced neurotoxicity.

15M S.A. Promoted the Formation of Non-toxic, Insoluble Aggregates during Aβ42 Oligomerization—The ThT and Western blotting analysis described above indicated that the 15M S.A. peptide reduced the formation of soluble Aβ42 oligomers (Fig. 1, *A* and *B*). However, we noticed a corresponding increase in the formation of non-toxic, insoluble material when Aβ42 was incubated in the presence of the 15M S.A. candidate. We hypothesized that the reduction in soluble Aβ42 may be concomitant with an increase in insoluble Aβ42 and used denaturing SDS-PAGE and Western blotting analysis to assess the relative amounts of soluble *versus* insoluble Aβ42 species. As in Fig. 1*B*, we found that the presence of 15M S.A. resulted in a dose-dependent reduction in soluble Aβ42 aggregates (Fig. 2*A*, *left panel*), whereas the control peptide resulted in similar soluble Aβ42 aggregates as the Aβ42 only sample (Fig. 2*A*, *left panel*). Increasing concentrations of 15M S.A. peptide resulted in increasing amounts of insoluble material, whereas no insoluble deposits were seen for the Aβ42 only sample, or in the presence of the control peptide. Western blotting revealed that Aβ42 aggregates were indeed present in the insoluble deposits, and the dose-dependent reduction in soluble Aβ42 aggregates in the presence of 15M S.A. was concurrent with an increase in insoluble Aβ42 aggregates (Fig. 2*A*, *right panel*). The amounts of insoluble Aβ42 generated in the presence of the peptides were further characterized using denaturing SDS-PAGE, followed by Western blotting and densitometric analysis. Soluble Aβ42 was measured to quantify the effect as Aβ42, which does not remain in the soluble fraction is by definition insoluble and measurements made from the soluble fraction have greater

[6] R. K. Barr, L. Wijaya, M. Morici, and G. Verdile, unpublished observations.

Downloaded from http://www.jbc.org/ at CURTIN UNIV OF TECHNOLOGY (CAUL) on June 12, 2016

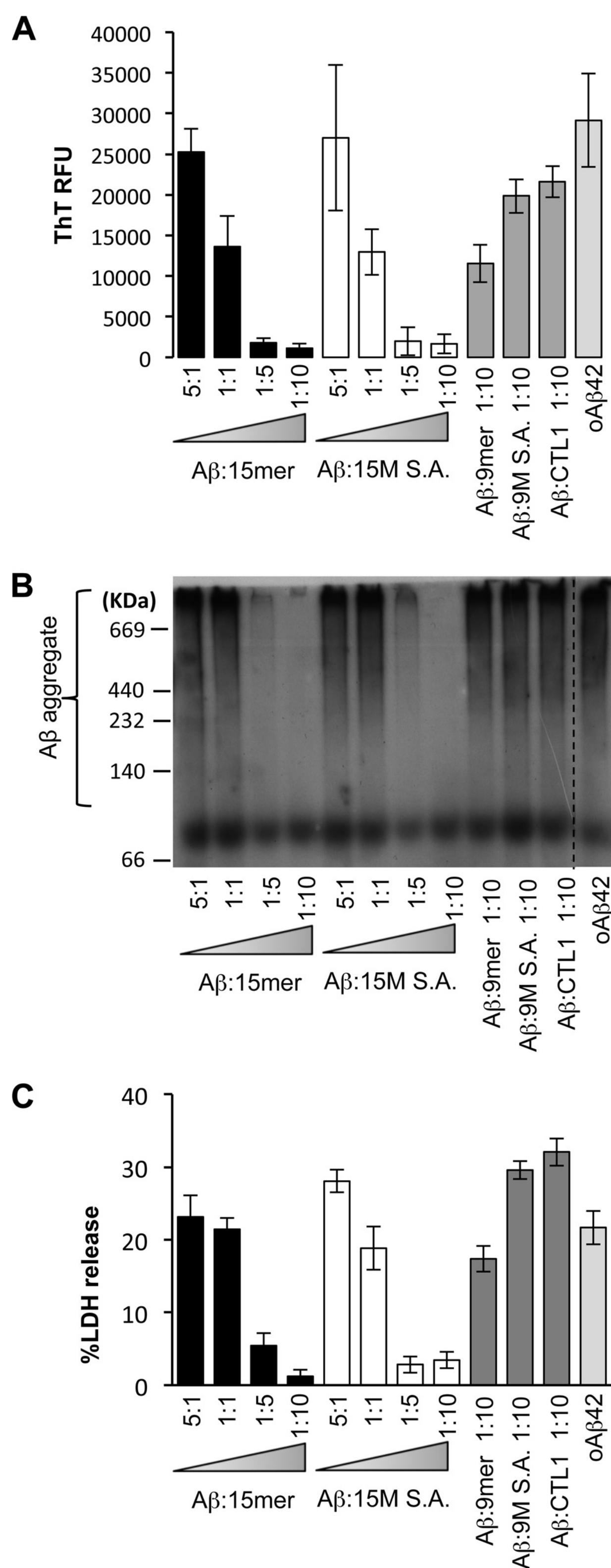

FIGURE 1. **Effects of candidate peptides on Aβ42 aggregation and neurotoxicity.** Aβ42 was incubated under conditions favoring oligomerization, in the presence or absence of the candidate peptides. At $t = 24$ h, samples were assayed for Aβ42 aggregation as measured by ThT relative fluorescence units (*RFU*) (*A,* mean ± S.D.) and Blue Native-PAGE/Western blotting for Aβ42 (*B*). The *dividing line* in *B* indicates that data has been spliced to simplify viewing, but all samples were from a single experiment. *C*, oligomeric Aβ42 stocks were diluted to 20 μM concentration and used to treat M17 neuroblastoma cells for 4 days. Aβ42-induced neurotoxicity was assessed by LDH release from the cells (mean ± S.D.). All data are from a single trial, but reflects the findings from at least 3 independent experiments.

accuracy and precision; measurements made from the insoluble fraction display elevated non-sedimenting background and variance, attributable to small amounts of residual/surface contamination after supernatant removal from the pellet (where present). As before, dose-dependent effects of the 15-mer and 15M S.A. peptides were observed, with increasing amounts shifting Aβ42 of the soluble fraction and into the insoluble fraction. The maximal effect was seen in the presence of 15M S.A. peptide at the 1:10 ratio, where one-fourth of Aβ42 remained in the soluble fraction (Fig. 2*C*). The amount of insoluble material present was also assayed, and whereas, as expected, non-sedimenting background was observable, the amount of Aβ42 in this fraction increased in line with decreases seen in the soluble fraction and the presence of observable pellets of insoluble material (Fig. 2*C*).

The utility of denaturing SDS-PAGE for analysis of Aβ assemblies is somewhat limited, given that most protein complexes and oligomers dissociate when treated with SDS, and thus observation of monomers and low-molecular weight oligomers by SDS-PAGE does not reveal whether larger assemblies existed prior to SDS addition (33). Thus, we chose to better characterize the soluble and insoluble Aβ assemblies formed in the presence of 15M S.A. using AFM. We found that Aβ42 oligomers formed in the absence of 15M S.A. were predominantly 1.5–4 nm in diameter, with a few larger aggregates 8–12 nm in diameter (Fig. 2*B*, *left panel*). However, Aβ assemblies formed in the presence of 15M S.A. ranged from smaller (2–6 nm diameter) to extreme (25–30 nm) size (Fig. 2*B*, *center panel*). The absence of aggregates in the presence of 15M S.A. only (Fig. 2*B*, *right panel*) suggests that aggregation of this peptide does not contribute to formation of larger Aβ assemblies. Taken together, it appears that the 15M S.A. peptide binds Aβ42, alters its oligomerization, and promotes the formation of non-toxic amorphous aggregates.

15M S.A. Binds Pre-formed Aβ42 Oligomers, as Shown by Surface Plasmon Resonance/Biacore and Coimmunoprecipitation Assays—The above assays indicated that 15M S.A. could influence the formation of Aβ42 oligomers. We next extended these findings by demonstrating that 15M S.A. could also interact with pre-formed Aβ42 oligomers (oAβ42) using two complementary measures of protein-protein interactions; surface plasmon resonance/Biacore assays and coimmunoprecipitation analysis. For these assays, we utilized two stable analogue control peptides (CTL1 S.A. and CTL2 S.A., "Experimental Procedures"), which were validated in ThT and LDH assays and found to mimic the activity of the CTL1 peptide used in our previous assays.[6] For surface plasmon resonance assays, 15M S.A. was immobilized on a Biacore sensorchip and oAβ42 concentrations over 5–40 μM were injected and monitored for binding to 15M S.A. It was evident that oAβ42 bound 15M S.A. in a dose-dependent manner (Fig. 3*A*). To confirm the specificity of this interaction, we next performed solution competition assays where free 15M S.A. peptide or control peptides were co-injected with oAβ42. For these studies, we used an oAβ42

Downloaded from http://www.jbc.org/ at CURTIN UNIV OF TECHNOLOGY (CAUL) on June 12, 2016

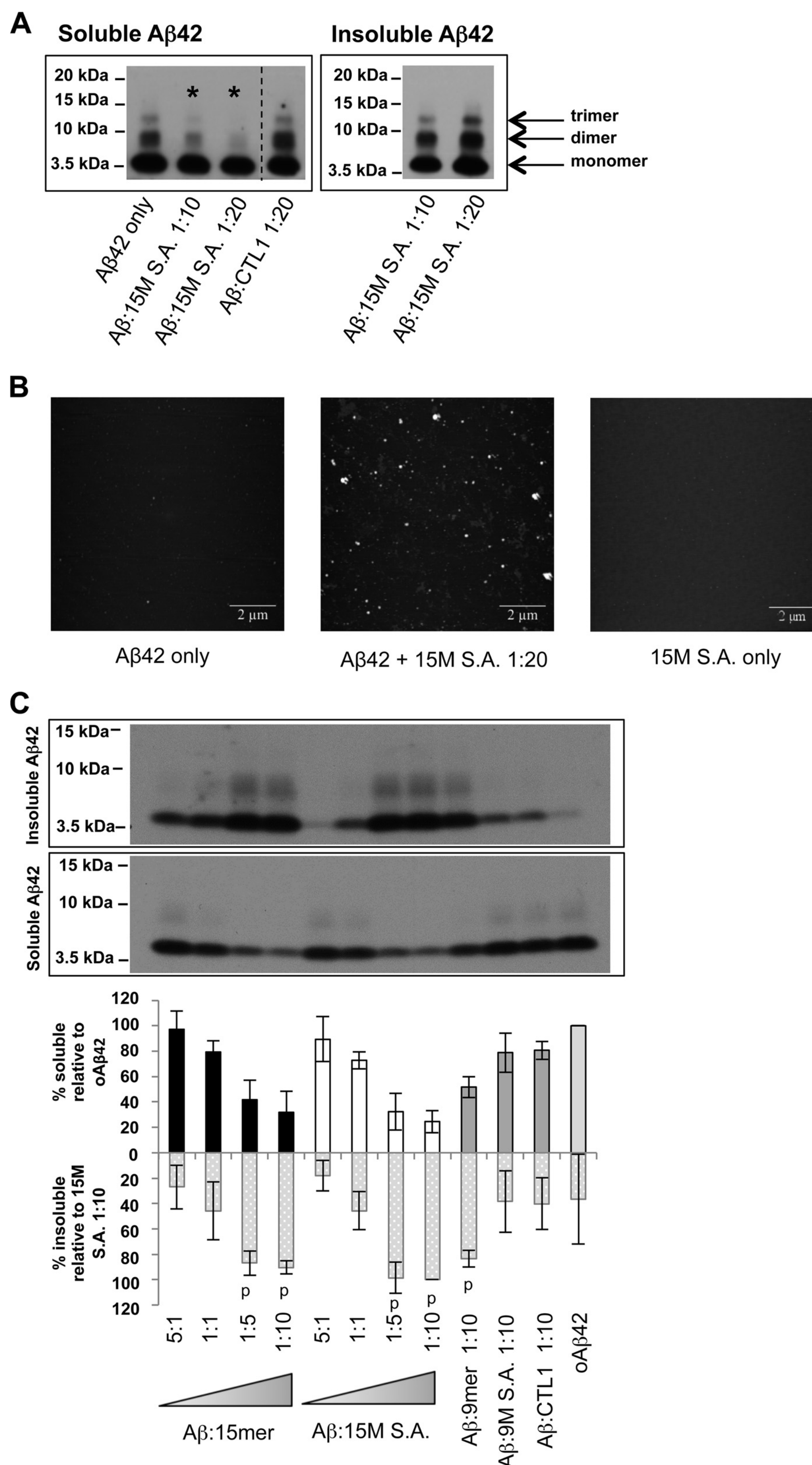

FIGURE 2. **15M S.A. reduced the formation of soluble Aβ42 oligomers and concurrently increased the formation of insoluble Aβ42 aggregates.** Aβ42 was incubated under conditions favoring oligomerization, in the presence or absence of 15M S.A. or control peptides at the indicated molar ratios. At $t = 24$ h, soluble and insoluble fractions (where present) were assayed for the presence of Aβ42 by SDS-PAGE and Western blotting (*A*, $n = 3$). The *asterisks* indicate samples with a reduction in soluble Aβ42 aggregates. The *dividing line* indicates that data has been spliced to simplify viewing, but all samples were from a single experiment. *B*, AFM of combined soluble/insoluble Aβ42 aggregates formed in the presence or absence of the 15M S.A. peptide under conditions favoring oligomerization ($n = 2$). *C*, SDS-PAGE and Western blotting results quantifying shift from soluble to insoluble Aβ42. A representative blot of reduced soluble Aβ42 is shown above the corresponding quantified results of 3 experiments, each with gels run in duplicate (mean ± S.D.). *Spotted bars* show insoluble Aβ42. The "p" marker indicates samples in which a small pellet of insoluble material could be observed by careful inspection.

Downloaded from http://www.jbc.org/ at CURTIN UNIV OF TECHNOLOGY (CAUL) on June 12, 2016

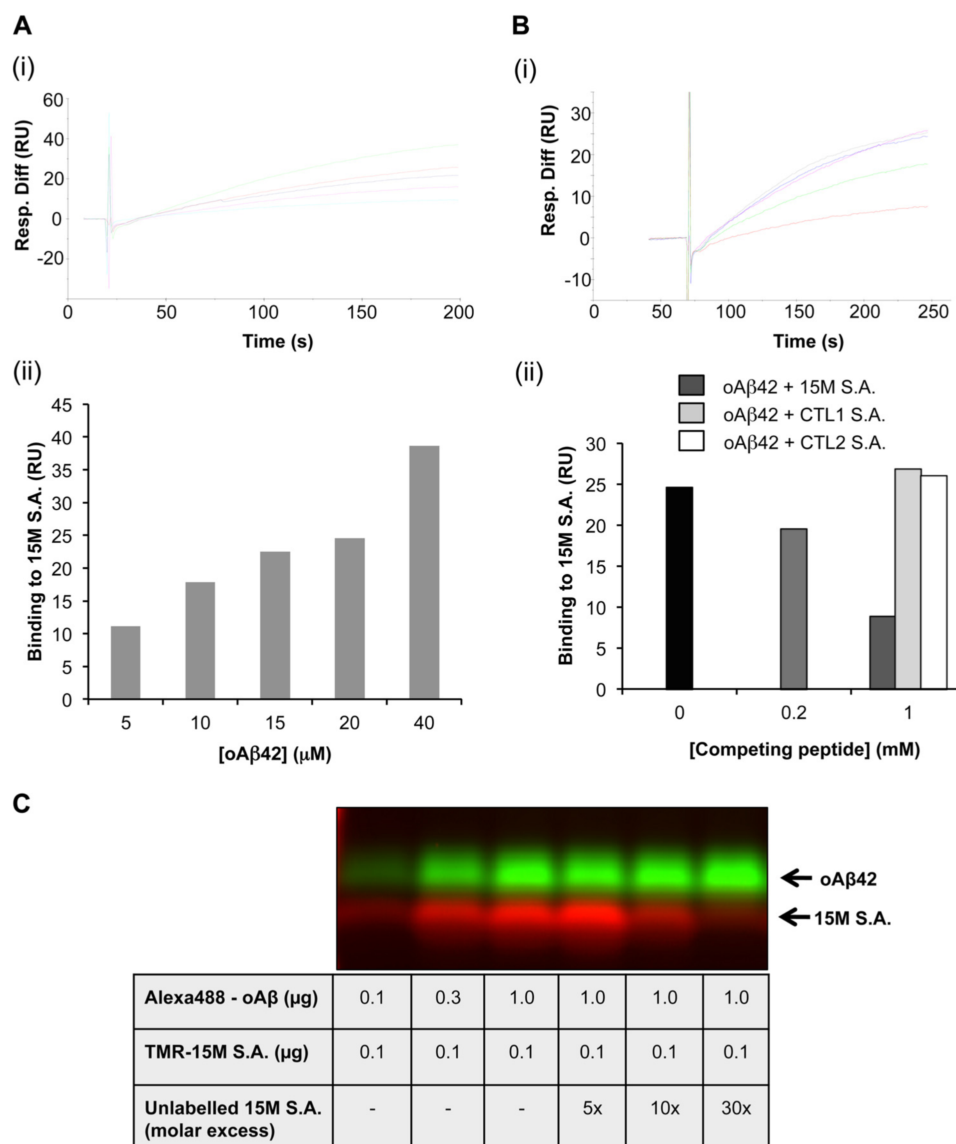

Alexa488 - oAβ (μg)	0.1	0.3	1.0	1.0	1.0	1.0
TMR-15M S.A. (μg)	0.1	0.1	0.1	0.1	0.1	0.1
Unlabelled 15M S.A. (molar excess)	-	-	-	5x	10x	30x

FIGURE 3. **15M S.A. binds pre-formed Aβ42 oligomers, as shown by surface plasmon resonance and coimmunoprecipitation assays.** A Biacore/SPR experiment (sensorgrams showing blank-subtracted response (*Resp. Diff*) (i) and bar chart of maximal response (ii)) illustrates dose-dependent binding of Aβ42 oligomers (oAβ42) to immobilized 15M S.A. peptide on a CM5 sensorchip surface (*A, single trial illustrated, n* = 3). Concentrations of oAβ42 injected were 5, 10, 15, 20, and 40 μM. *B*, competition assay indicating that binding between oAβ42 (20 μM) and immobilized 15M S.A. was effectively disrupted by free 15M S.A. in solution, but not equivalent concentrations of two control peptides (CTL1 S.A. and CTL2 S.A.) (*single trial illustrated*, *n* = 2). *C*, coimmunoprecipitation experiment with Alexa 488-labeled oAβ42 captured using 6E10 antibody and detection of bound TMR-labeled 15M S.A. peptide. Immunocomplexes were separated by denaturing SDS-PAGE and fluorescently labeled proteins were visualized using a Typhoon imaging system. TMR-15M S.A. peptide was bound by Alexa 488-Aβ42 in a concentration-dependent manner, which could be reduced by the presence of an excess of unlabeled 15M S.A. peptide in solution (*n* = 2).

concentration of 20 μM, which was found to give reproducible responses in replicate injections over multiple cycles in a given experiment. We found that increasing concentrations of free 15M S.A. in solution resulted in a dose-dependent reduction in oAβ42 binding the immobilized 15M S.A. on the sensorchip (Fig. 3*B*). However, equivalent concentrations of two different control peptides could not mimic this action and did not reduce the amount of oAβ42 binding to immobilized 15M S.A. (Fig. 3*B*). To confirm these findings, we performed complementary studies involving coimmunoprecipitation analysis. Here, Alexa 488-labeled oAβ42 was incubated with TMR-labeled 15M S.A. peptide to promote the formation of a protein complex, which was captured by immunoprecipitation using 6E10 antibody to bind oAβ species. Denaturing SDS-PAGE was used to separate the protein complexes and oAβ42 and 15M S.A. were visualized via their respective fluorescent labels. The 15M S.A. peptide coimmunoprecipitated with oAβ42 in a dose-dependent manner (Fig. 3*C*). Furthermore, the amount of labeled, coimmunoprecipitated 15M S.A. peptide could be reduced by competition in solution with increasing quantities of unlabeled 15M S.A. peptide (Fig. 3*C*). These findings confirmed the results of the surface plasmon resonance assays and collectively indicate that the 15M S.A. peptide directly interacts with oAβ42.

We extended the surface plasmon resonance analysis to obtain an estimate of the affinity of the interaction between 15M S.A. and oAβ42, by fitting the experimental data to models within the BiaEvaluation v4.1 software. It is crucial to highlight that this value is only an overall estimate of binding affinity

Downloaded from http://www.jbc.org/ at CURTIN UNIV OF TECHNOLOGY (CAUL) on June 12, 2016

across the entire spectrum of oligomers present in the oAβ42 preparation, which is a heterogeneous mixture of aggregates. The best fit occurred for a 1:1 binding model with drifting baseline correction (χ^2 = 0.214) and yielded a K_D value of low micromolar value (11 μM), indicating a moderate affinity between the 15M S.A. peptide and oAβ42, and similar to other reports of Aβ-peptide interactions (34).

15M S.A. Binds Monomeric, Oligomeric, and Fibrillar Aβ42 in Biacore Assays—Thus far, we had demonstrated that 15M S.A. could influence oligomer formation and directly bind preformed oAβ42. We further investigated the ability of this peptide to bind less aggregated Aβ preparations (monomeric (m) Aβ42) and more aggregated preparations (fibrillar (f) Aβ42). To allow a comparison of 15M S.A. binding to different Aβ species, a sensorchip was generated with immobilized monomeric, oligomeric, and fibrillar Aβ42 preparations as described under "Experimental Procedures." A series of 15M S.A. concentrations were injected across the surfaces, monitored for binding to the respective Aβ42 species, and the data were corrected for the relative amount of immobilized material on the individual flow cells. We found that 15M S.A. interacted with all of the Aβ42 species in a concentration-dependent manner, but the highest magnitude of binding was seen for the Aβ42 fibrils (Fig. 4). This most likely reflects the fact that the Aβ42 fibrils have multiple binding sites for 15M S.A., given that they are composed of repeating units of monomeric Aβ42. Overall, this data shows that the 15M S.A. peptide is able to bind unaggregated, monomeric Aβ42 (perhaps accounting for its earlier effects (Fig. 1) in reducing the formation of oAβ42) as well as oligomeric and fibrillar Aβ42 assemblies. The binding of 15M S.A. to more mature amyloid species was investigated further below.

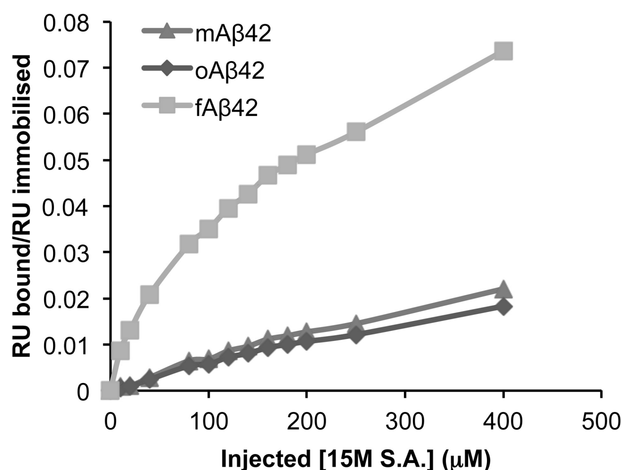

FIGURE 4. **15M S.A. binds monomeric, oligomeric, and fibrillar Aβ42.** Aβ42 was incubated under conditions favoring formation of monomers (mAβ42), oligomers (oAβ42), or fibrils (fAβ42) as described under "Experimental Procedures." These were immobilized on individual flow cells of a CM5 sensorchip, where an unmodified surface was reserved for blank-subtraction. A series of concentrations of 15M S.A. peptide were injected across these surfaces and monitored for binding. In each case, the binding response was corrected for the relative quantity of immobilized material (RU bound/RU immobilized). 15M S.A. bound all of the immobilized Aβ42 assemblies, with the highest binding response observed for Aβ42 fibrils.

15M S.A. Can Detect Amyloid Plaques in ex Vivo Immunohistochemical Staining of AD Brain Slices—Given the ability of 15M S.A. to interact with Aβ42 fibrils, we extended this finding to investigate whether TMR-labeled 15M S.A. could be used to stain amyloid plaques *ex vivo* using brain tissue sections from AD model mice, in comparison with thioflavin S, which binds mature amyloid deposits and readily detects these plaques. In *ex vivo* staining of brain tissue from 8-month-old 5xFAD AD model mice, thioflavin S staining revealed extensive plaques within the brain (Fig. 5*A*). In comparison, serial sections treated with the TMR-labeled 15M S.A. peptide also resulted in staining of some amyloid deposits, but to a lesser extent than thio-

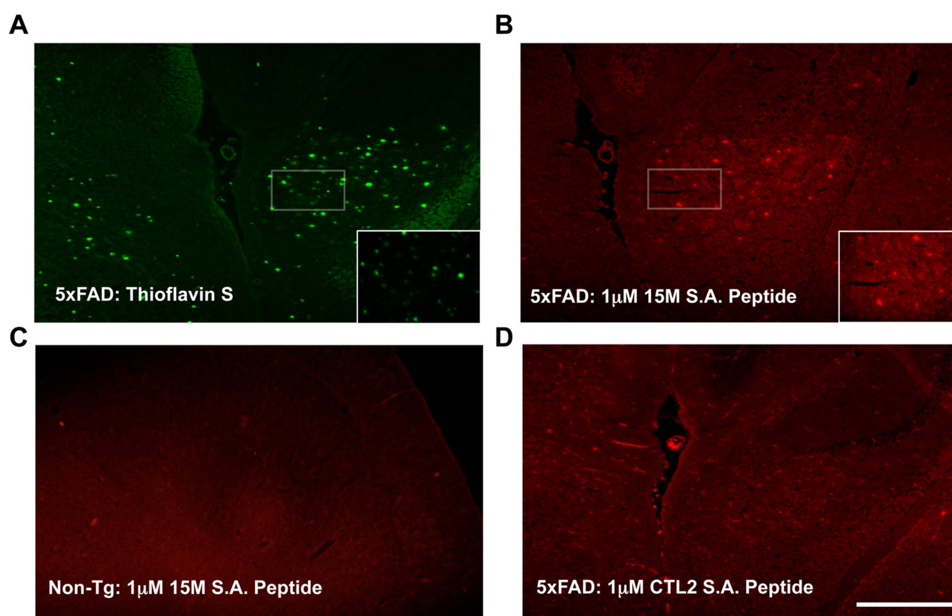

FIGURE 5. **15M S.A. binds amyloid deposits in brain tissue from the 5xFAD mouse model of AD**. *Ex vivo* staining of serial sagittal sections from the subiculum of 8-month-old AD model mice (5xFAD) or age-matched non-transgenic controls (*Non-Tg*) (10 mM thickness, ×10 magnification, *scale bar* = 200 mm; *inset* = ×40 magnification) is shown. *A*, amyloid deposits as detected by thioflavin S staining. *B*, TMR-labeled 15M S.A. peptide bound a subset of the total amyloid deposits. *C*, TMR-labeled 15M S.A. peptide did not stain equivalent brain tissue from Non-Tg control mice. *D*, TMR-labeled control peptide (*CTL2 S.A.*) did not result in any detectable staining of amyloid deposits in 5xFAD brain tissue (*n* = 2).

Downloaded from http://www.jbc.org/ at CURTIN UNIV OF TECHNOLOGY (CAUL) on June 12, 2016

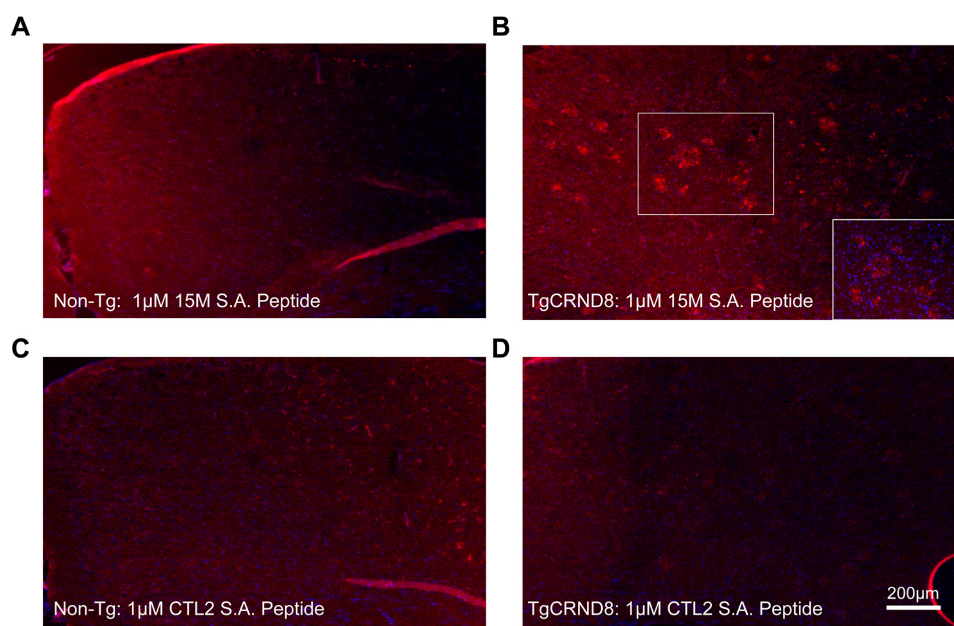

FIGURE 6. **15M S.A. binds amyloid deposits in brain tissue from the TgCRND8 mouse model of AD.** *Ex vivo* staining of serial coronal sections from the whole brain of 8-month-old AD model mice (*TgCRND8*) or age-matched non-transgenic controls (*Non-Tg*) (10-μm thickness, $\times$5 magnification, *scale bar* = 200 μm; *inset* = $\times$10 magnification) is shown. DAPI was used as a nuclear counterstain. *A,* TMR-labeled 15M S.A. peptide did not stain cortical brain tissue from Non-Tg control mice. *B,* TMR-labeled 15M S.A. peptide bound to amyloid deposits in TgCRND8 cortical brain tissue. *C* and *D,* TMR-labeled control peptide (CTL2 S.A.) did not result in any detectable staining of amyloid deposits in Non-Tg or TgCRND8 brain tissue (n = 1).

flavin S (Fig. 5*B*). Notably, the TMR-labeled 15M S.A. peptide did not stain control (non-AD) brain tissue from age-matched control mice in related experiments (Fig. 5*C*). Additionally, a TMR-labeled control peptide did not result in any comparable staining of amyloid deposits in the 5xFAD brain tissue (Fig. 5*D*). These findings were replicated in brain tissue from another transgenic AD mouse model, the TgCRND8 (Fig. 6). The TMR-labeled 15M S.A. peptide (Fig. 6*B*), but not the control (CTL2 S.A., Fig. 6*D*) peptide, stained amyloid deposits in TgCRND8 brain tissue but not in tissue from non-transgenic littermates (Fig. 6*A*). These data in brain tissue from two independent AD mouse models indicate that, in addition to binding Aβ42 monomers, oligomers, and fibrils *in vitro*, 15M S.A. was also capable of binding mature amyloid deposits in brain tissue *ex vivo*.

Tritiated 15M S.A. Peptide Is Detected in the Brains of Mice following Intravenous Administration—The demonstration of binding of the 15M S.A. peptide to aggregated Aβ42 *in vitro* and *ex vivo* suggested it may also have the potential to bind Aβ42 *in vivo*. However, the blood-brain barrier (BBB) represents a major hurdle for the delivery of molecules into the brain from the periphery. To make a preliminary assessment of the ability of the 15M S.A peptide to cross the BBB *in vivo*, 10 μCi of tritiated peptide was administered by intravenous injection to mice as described under "Experimental Procedures," and its concentration in brain and plasma was determined in samples collected over a 0.5–4 h period. Scintillation counting revealed that the plasma concentrations of tritiated peptide decreased with time, as expected following intravenous administration. However, the tritiated peptide was detected in brain homogenate at the initial t = 30 min time point and remained relatively constant until t = 4 h, suggesting that the peptide remains stable in the brain (Fig. 7*A*). We further performed control experiments to ensure that the measured radioactivity in brain and plasma samples corresponded to intact ^{3}H-15M S.A. peptide, rather than free label or degradation products (Fig. 7, *B* and *C*). There was no apparent shift in the retention time of ^{3}H-labeled 15M S.A. in brain and plasma samples collected at designated time points, suggesting that the majority of detected radioactivity was associated with intact peptide. This provided initial evidence that the 15M S.A. peptide can cross the blood-brain barrier *in vivo* following intravenous administration and potentially access brain-based Aβ42 targets.

Discussion

Here, we extend our earlier findings (1) and report the generation of a 15-mer stable analogue peptide that targets Aβ42. We provide evidence that the peptide is multifaceted in its actions, in that it can bind monomeric, oligomeric, and fibrillar Aβ42 and also reduce the formation of neurotoxic Aβ42 oligomers.

The ability of the 15M S.A. peptide to interfere with formation of oligomers is of particular interest, given their likely role in mediating the neurotoxicity of Aβ42. We noted that in the presence of 15M S.A., the formation of soluble Aβ42 oligomers was decreased, with a concurrent increase in the formation of non-toxic, amorphous aggregates. Thus, it appears that the 15M S.A. peptide can shift the equilibrium between different Aβ42 assemblies and favor the formation of non-toxic, amorphous aggregates rather than soluble oligomers. A recent report demonstrated that the aggregation of Aβ42 is promoted by a positive feedback loop that originates from the interactions between the monomeric and fibrillar forms of this peptide (35). More specifically, once a small but critical concentration of amyloid fibrils has accumulated, the toxic oligomeric species are predominantly formed from monomeric peptide molecules through a fibril-catalyzed secondary nucleation reaction (35).

Downloaded from http://www.jbc.org/ at CURTIN UNIV OF TECHNOLOGY (CAUL) on June 12, 2016

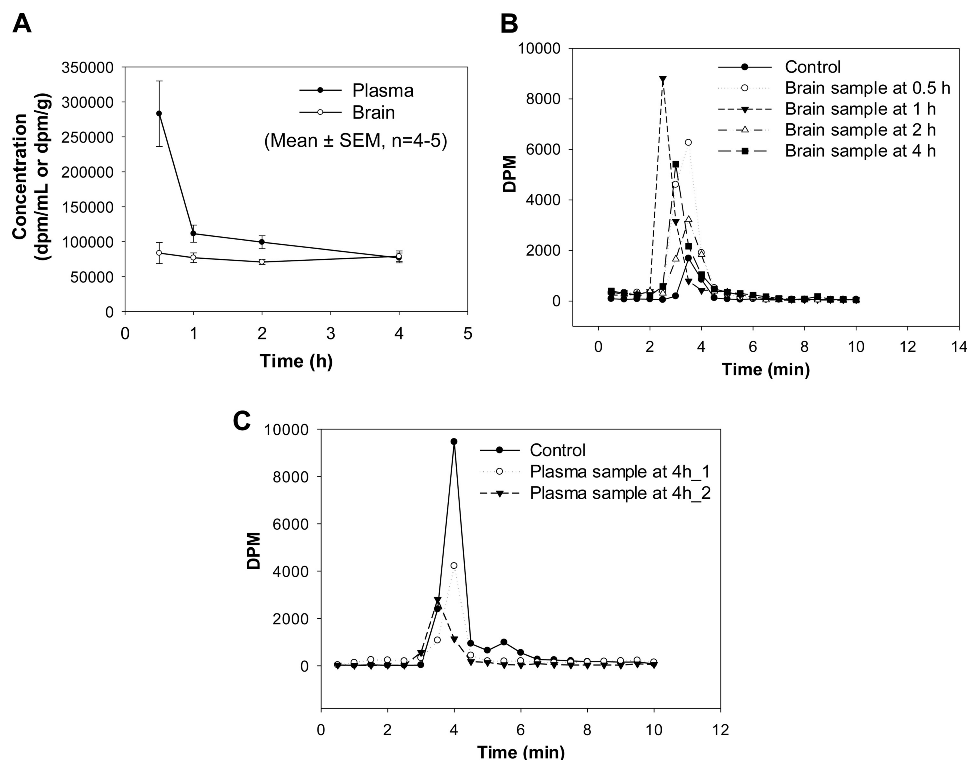

FIGURE 7. **Tritiated 15M S.A. peptide is detected in the brains of mice following intravenous administration.** Male Swiss Outbred mice were administered 10 μCi of ^{3}H-labeled 15M S.A. peptide by tail vein injection. Brain and plasma samples were collected over a 0.5–4-h period and the determination of compound in plasma and brain homogenate was performed by liquid scintillation counting (*A, n* = 3). Data are mean ± S.E. *B* and *C*, assessment of the intactness of ^{3}H-15M S.A. peptide in samples from brain (*B*) and plasma (*C*), respectively. HPLC/scintillation counting indicated a similar retention time for radioactivity detected in brain/plasma samples, and undegraded ^{3}H-labeled 15M S.A. peptide (*Control*), suggesting that the majority of detected radioactivity in samples was due to intact peptide.

Given our data showing that 15M S.A. binds monomers and fibrils, it is feasible that it could interfere with such a nucleation reaction. Further validation is required to determine whether 15M S.A. can inhibit the formation of soluble Aβ42 oligomers via interactions with monomers, fibrils, or a combination of these Aβ42 moieties.

The ability of 15M S.A. to bind preformed Aβ42 oligomers is also highly significant, particularly with respect to developing agents that target early events in the disease process. As mentioned earlier, the formation of soluble aggregates is thought to occur prior to plaque and tangle formation and promote the neurodegenerative process. Current evidence suggests that Aβ deposition may precede mild cognitive impairment (the first clinical manifestation of AD) by 10–20 years (36–38) and so the accumulation of Aβ oligomers could occur more than 20 years prior to the development of a clinical AD phenotype. It would be advantageous to have the ability to image some of the earliest events in the development of AD, when therapeutic approaches to neutralize and/or clear neurotoxic oligomers might prevent the resulting neuronal injury and cognitive decline. Given the multifaceted action of 15M S.A. in inhibiting oligomer formation and binding preformed oligomers, it may prove useful in both diagnostic and therapeutic approaches targeting preclinical AD.

Peptide-based drugs offer several advantages compared with other popular alternatives, including antibodies. Their small size means they can be produced at a lower cost, with higher activity per mass and often less immunogenicity (39). A further hurdle for antibody-based approaches is penetration of the BBB, which allows only ~0.1% of peripheral antibody to gain access to the central nervous system (40) and thus smaller peptides may be more amenable to BBB transport. Certainly, our preliminary data presented here suggests that the 15M S.A. peptide is capable of crossing the BBB *in vivo* to some degree (Fig. 7). Furthermore, a recent study designed short 20-mer peptides to bind the C terminus of APP-C99 and following intraperitoneal injection of mice showed efficacy at reducing cerebral Aβ levels (41), providing initial evidence for the potential of similar sized peptides to cross the BBB. In our ongoing studies, we are further investigating the extent of BBB transport of 15M S.A. and its ability to bind Aβ42 aggregates *in vivo*, to better define its diagnostic and therapeutic capabilities.

Several peptide-based agents have been designed to target Aβ and inhibit its aggregation. Many of these peptides can reduce Aβ aggregation and neurotoxicity *in vitro* and modified versions with improved stability have further been shown to be effective *in vivo* (*e.g.* Ref. 26 and 42–49). Other peptides that have recently been reported to target oligomeric Aβ in particular include a peptide based on the N-terminal fragment of the cellular prion protein (N1) that blocked the formation of amyloid fibrils *in vitro* and bound Aβ42 oligomers and inhibited their neurotoxicity *in vivo* (50) and the ABP-p-4–5 synthetic peptide corresponding to a region of the human pericentriolar material 1 protein that preferentially bound Aβ42 oligomers and protected against their neurotoxicity *in vitro* (51). Few of

Downloaded from http://www.jbc.org/ at CURTIN UNIV OF TECHNOLOGY (CAUL) on June 12, 2016

these agents have progressed to the clinic, often as a result of undesirable effects (insolubility, toxicity) at the relatively high doses required to observe their protective effects. However, it is feasible that this may be circumvented by chemical modifications such as conjugation with polyethylene glycol, which can improve solubility, increase circulatory half-life, reduce immunogenicity, and improve delivery (52–54). Targeted delivery methods may also improve the efficacy of peptide agents to cross the BBB, such as "Trojan horse" approaches (55) and liposomal nanoparticles (56). Another approach to enhance BBB transport is to periodically and reversibly modulate tight junctions. This has recently been demonstrated through the use of siRNA directed against claudin-5 (57).

Although dose limitations have tended to preclude the use of peptides as therapeutic and preventative agents thus far, their high specificity in binding to the Aβ42 target may render them useful as diagnostic AD imaging probes, where only tracer quantities are required. The ability of fluorescently tagged 15M S.A. to bind fibrillar Aβ42 *in vitro*, and amyloid plaques *ex vivo*, highlights its potential as an AD imaging agent. However, detection of mature amyloid plaques can already be achieved by positron emission tomography imaging with current amyloid imaging agents such as the "gold-standard" Pittsburg compound B (58) (a radiolabeled analogue of ThT) and newer ^{18}F analogues (*e.g.* Refs. 59 and 60). It is important to highlight here that the existing amyloid imaging tracers are unable to detect oligomeric Aβ42. Although oligomer-specific antibodies have been identified (61, 62), antibody-based positron emission tomography imaging has not proved useful due to poor brain penetration of the probes (63). Here, we have used several biochemical assays to indicate that the 15M S.A. peptide can indeed bind oligomeric Aβ42. Thus, it seems feasible that when conjugated to an appropriate radioisotopic tracer (*e.g.* ^{18}F), 15M S.A. has the potential to bridge an important gap in the existing diagnostic techniques and non-invasively highlight the presence of oligomeric Aβ42 *in vivo*.

In our ongoing studies, we are attempting to clarify the binding sites on the 15M S.A. and Aβ42 peptides that mediate their interaction. This may clarify how 15M S.A. binds monomeric and aggregated Aβ42 and reduces the formation of toxic Aβ42 oligomers *in vitro*, as reported here. It may further indicate other mechanisms by which 15M S.A. might be neuroprotective with respect to Aβ42-induced toxicity *in vivo*. For example, specific domains of Aβ have been reported to facilitate aggregation on and association with lipid bilayers, with implications for bilayer stability and cell viability (64). Thus, if 15M S.A. can make contact with such Aβ42 domains and interrupt lipid binding, this could potentially result in neuroprotection. Finally, clarification of the binding interface between 15M S.A. and Aβ42 may assist in the design of novel peptidomimetics that mimic the action of 15M S.A. and better satisfy the physicochemical requirements associated with *in vivo* therapeutics.

Overall, we have validated and characterized the binding profile of a novel Aβ binding peptide that has the potential to bridge an important gap in the existing diagnostic techniques and permit timely intervention to reduce or prevent the neurodegeneration and cognitive decline associated with the accumulation of oligomeric Aβ42.

Author Contributions—R. M. conceived the study and together with G. V., K. T. and R. K. B. co-ordinated the study. R. K. B. and G. V. wrote the manuscript. R. K. B., L. K. W., M. M., V. G., and S. P. performed and analyzed the experiments in Figs. 1–5. L. J. and J. A. N. conceived, performed, and analyzed experiments in Fig. 7. P. E. F. conceived, performed, and analyzed experiments in Table 1. P. E. F. and E. K. performed experiments in Fig. 6. All authors reviewed the results and approved the final version of the manuscript.

Acknowledgments—We thank Ling Wu (University of Toronto) for performing the assays to measure peptide stability in brain homogenate and Prof. Colin Masters (University of Melbourne, Australia) for kindly providing the WO2 antibody.

References

1. Taddei, K., Laws, S. M., Verdile, G., Munns, S., D'Costa, K., Harvey, A. R., Martins, I. J., Hill, F., Levy, E., Shaw, J. E., and Martins, R. N. (2010) Novel phage peptides attenuate β amyloid-42 catalysed hydrogen peroxide production and associated neurotoxicity. *Neurobiol. Aging* **31,** 203–214
2. Evans, D. A., Funkenstein, H. H., Albert, M. S., Scherr, P. A., Cook, N. R., Chown, M. J., Hebert, L. E., Hennekens, C. H., and Taylor, J. O. (1989) Prevalence of Alzheimer's disease in a community population of older persons: higher than previously reported. *JAMA* **262,** 2551–2556
3. Burdick, D., Soreghan, B., Kwon, M., Kosmoski, J., Knauer, M., Henschen, A., Yates, J., Cotman, C., and Glabe, C. (1992) Assembly and aggregation properties of synthetic Alzheimer's A4/β amyloid peptide analogs. *J. Biol. Chem.* **267,** 546–554
4. Jarrett, J. T., Berger, E. P., and Lansbury, P. T., Jr. (1993) The carboxy terminus of the β amyloid protein is critical for the seeding of amyloid formation: implications for the pathogenesis of Alzheimer's disease. *Biochemistry* **32,** 4693–4697
5. Ono, K., and Yamada, M. (2011) Low-n oligomers as therapeutic targets of Alzheimer's disease. *J. Neurochem.* **117,** 19–28
6. Lambert, M. P., Barlow, A. K., Chromy, B. A., Edwards, C., Freed, R., Liosatos, M., Morgan, T. E., Rozovsky, I., Trommer, B., Viola, K. L., Wals, P., Zhang, C., Finch, C. E., Krafft, G. A., and Klein, W. L. (1998) Diffusible, nonfibrillar ligands derived from Aβ1–42 are potent central nervous system neurotoxins. *Proc. Natl. Acad. Sci. U.S.A.* **95,** 6448–6453
7. Nimmrich, V., Grimm, C., Draguhn, A., Barghorn, S., Lehmann, A., Schoemaker, H., Hillen, H., Gross, G., Ebert, U., and Bruehl, C. (2008) Amyloid β oligomers (Aβ(1–42) globulomer) suppress spontaneous synaptic activity by inhibition of P/Q-type calcium currents. *J. Neurosci.* **28,** 788–797
8. Walsh, D. M., Hartley, D. M., Kusumoto, Y., Fezoui, Y., Condron, M. M., Lomakin, A., Benedek, G. B., Selkoe, D. J., and Teplow, D. B. (1999) Amyloid β-protein fibrillogenesis: structure and biological activity of protofibrillar intermediates. *J. Biol. Chem.* **274,** 25945–25952
9. Ono, K., Naiki, H., and Yamada, M. (2006) The development of preventives and therapeutics for Alzheimer's disease that inhibit the formation of β-amyloid fibrils (fAβ), as well as destabilize preformed fAβ. *Curr. Pharm. Des.* **12,** 4357–4375
10. Näslund, J., Haroutunian, V., Mohs, R., Davis, K. L., Davies, P., Greengard, P., and Buxbaum, J. D. (2000) Correlation between elevated levels of amyloid β-peptide in the brain and cognitive decline. *JAMA* **283,** 1571–1577
11. Gong, Y., Chang, L., Viola, K. L., Lacor, P. N., Lambert, M. P., Finch, C. E., Krafft, G. A., and Klein, W. L. (2003) Alzheimer's disease-affected brain: presence of oligomeric Aβ ligands (ADDLs) suggests a molecular basis for reversible memory loss. *Proc. Natl. Acad. Sci. U.S.A.* **100,** 10417–10422
12. Cleary, J. P., Walsh, D. M., Hofmeister, J. J., Shankar, G. M., Kuskowski, M. A., Selkoe, D. J., and Ashe, K. H. (2005) Natural oligomers of the amyloid-β protein specifically disrupt cognitive function. *Nat. Neurosci.* **8,** 79–84

Downloaded from http://www.jbc.org/ at CURTIN UNIV OF TECHNOLOGY (CAUL) on June 12, 2016

13. Shankar, G. M., Bloodgood, B. L., Townsend, M., Walsh, D. M., Selkoe, D. J., and Sabatini, B. L. (2007) Natural oligomers of the Alzheimer amyloid-β protein induce reversible synapse loss by modulating an NMDA-type glutamate receptor-dependent signaling pathway. *J. Neurosci.* **27,** 2866–2875
14. Hung, L. W., Ciccotosto, G. D., Giannakis, E., Tew, D. J., Perez, K., Masters, C. L., Cappai, R., Wade, J. D., and Barnham, K. J. (2008) Amyloid-β peptide (Aβ) neurotoxicity is modulated by the rate of peptide aggregation: Aβ dimers and trimers correlate with neurotoxicity. *J. Neurosci.* **28,** 11950–11958
15. Shankar, G. M., Li, S., Mehta, T. H., Garcia-Munoz, A., Shepardson, N. E., Smith, I., Brett, F. M., Farrell, M. A., Rowan, M. J., Lemere, C. A., Regan, C. M., Walsh, D. M., Sabatini, B. L., and Selkoe, D. J. (2008) Amyloid-β protein dimers isolated directly from Alzheimer's brains impair synaptic plasticity and memory. *Nat. Med.* **14,** 837–842
16. Westerman, M. A., Cooper-Blacketer, D., Mariash, A., Kotilinek, L., Kawarabayashi, T., Younkin, L. H., Carlson, G. A., Younkin, S. G., and Ashe, K. H. (2002) The relationship between Aβ and memory in the Tg2576 mouse model of Alzheimer's disease. *J. Neurosci.* **22,** 1858–1867
17. Billings, L. M., Oddo, S., Green, K. N., McGaugh, J. L., and LaFerla, F. M. (2005) Intraneuronal Aβ causes the onset of early Alzheimer's disease-related cognitive deficits in transgenic mice. *Neuron* **45,** 675–688
18. Oddo, S., Caccamo, A., Kitazawa, M., Tseng, B. P., and LaFerla, F. M. (2003) Amyloid deposition precedes tangle formation in a triple transgenic model of Alzheimer's disease. *Neurobiol. Aging* **24,** 1063–1070
19. Ma, Q. L., Yang, F., Rosario, E. R., Ubeda, O. J., Beech, W., Gant, D. J., Chen, P. P., Hudspeth, B., Chen, C., Zhao, Y., Vinters, H. V., Frautschy, S. A., and Cole, G. M. (2009) β-Amyloid oligomers induce phosphorylation of Tau and inactivation of insulin receptor substrate via c-Jun N-terminal kinase signaling: suppression by omega-3 fatty acids and curcumin. *J. Neurosci.* **29,** 9078–9089
20. Tomiyama, T., Matsuyama, S., Iso, H., Umeda, T., Takuma, H., Ohnishi, K., Ishibashi, K., Teraoka, R., Sakama, N., Yamashita, T., Nishitsuji, K., Ito, K., Shimada, H., Lambert, M. P., Klein, W. L., and Mori, H. (2010) A mouse model of amyloid β oligomers: their contribution to synaptic alteration, abnormal Tau phosphorylation, glial activation, and neuronal loss *in vivo*. *J. Neurosci.* **30,** 4845–4856
21. Benilova, I., Karran, E., and De Strooper, B. (2012) The toxic Aβ oligomer and Alzheimer's disease: an emperor in need of clothes. *Nat. Neurosci.* **15,** 349–357
22. Stine, W. B., Jungbauer, L., Yu, C., and LaDu, M. J. (2011) Preparing synthetic Aβ in different aggregation states. *Methods Mol. Biol.* **670,** 13–32
23. Cerf, E., Gustot, A., Goormaghtigh, E., Ruysschaert, J. M., and Raussens, V. (2011) High ability of apolipoprotein E4 to stabilize amyloid-β peptide oligomers, the pathological entities responsible for Alzheimer's disease. *FASEB J.* **25,** 1585–1595
24. Binley, J. M., Lybarger, E. A., Crooks, E. T., Seaman, M. S., Gray, E., Davis, K. L., Decker, J. M., Wycuff, D., Harris, L., Hawkins, N., Wood, B., Nathe, C., Richman, D., Tomaras, G. D., Bibollet-Ruche, F., Robinson, J. E., Morris, L., Shaw, G. M., Montefiori, D. C., and Mascola, J. R. (2008) Profiling the specificity of neutralizing antibodies in a large panel of plasmas from patients chronically infected with human immunodeficiency virus type 1 subtypes B and C. *J. Virol.* **82,** 11651–11668
25. Miles, L. A., Wun, K. S., Crespi, G. A., Fodero-Tavoletti, M. T., Galatis, D., Bagley, C. J., Beyreuther, K., Masters, C. L., Cappai, R., McKinstry, W. J., Barnham, K. J., and Parker, M. W. (2008) Amyloid-β-anti-amyloid-β complex structure reveals an extended conformation in the immunodominant B-cell epitope. *J. Mol. Biol.* **377,** 181–192
26. Taylor, M., Moore, S., Mayes, J., Parkin, E., Beeg, M., Canovi, M., Gobbi, M., Mann, D. M., and Allsop, D. (2010) Development of a proteolytically stable retro-inverso peptide inhibitor of β-amyloid oligomerization as a potential novel treatment for Alzheimer's disease. *Biochemistry* **49,** 3261–3272
27. Jungbauer, L. M., Yu, C., Laxton, K. J., and LaDu, M. J. (2009) Preparation of fluorescently-labeled amyloid-β peptide assemblies: the effect of fluorophore conjugation on structure and function. *J. Mol. Recognit.* **22,** 403–413
28. Oakley, H., Cole, S. L., Logan, S., Maus, E., Shao, P., Craft, J., Guillozet-Bongaarts, A., Ohno, M., Disterhoft, J., Van Eldik, L., Berry, R., and Vassar, R. (2006) Intraneuronal β-amyloid aggregates, neurodegeneration, and neuron loss in transgenic mice with five familial Alzheimer's disease mutations: potential factors in amyloid plaque formation. *J. Neurosci.* **26,** 10129–10140
29. Drummond, E. S., Muhling, J., Martins, R. N., Wijaya, L. K., Ehlert, E. M., and Harvey, A. R. (2013) Pathology associated with AAV mediated expression of β amyloid or C100 in adult mouse hippocampus and cerebellum. *PLoS ONE* **8,** e59166
30. Youmans, K. L., Tai, L. M., Nwabuisi-Heath, E., Jungbauer, L., Kanekiyo, T., Gan, M., Kim, J., Eimer, W. A., Estus, S., Rebeck, G. W., Weeber, E. J., Bu, G., Yu, C., and Ladu, M. J. (2012) APOE4-specific changes in Aβ accumulation in a new transgenic mouse model of Alzheimer disease. *J. Biol. Chem.* **287,** 41774–41786
31. Jin, L., Li, J., Nation, R. L., and Nicolazzo, J. A. (2011) Impact of P-glycoprotein inhibition and lipopolysaccharide administration on blood-brain barrier transport of colistin in mice. *Antimicrob. Agents Chemother.* **55,** 502–507
32. Bergström, C. A., Charman, S. A., and Nicolazzo, J. A. (2012) Computational prediction of CNS drug exposure based on a novel *in vivo* dataset. *Pharm. Res.* **29,** 3131–3142
33. Bitan, G., Fradinger, E. A., Spring, S. M., and Teplow, D. B. (2005) Neurotoxic protein oligomers: what you see is not always what you get. *Amyloid* **12,** 88–95
34. Funke, S. A., Bartnik, D., Glück, J. M., Piorkowska, K., Wiesehan, K., Weber, U., Gulyas, B., Halldin, C., Pfeifer, A., Spenger, C., Muhs, A., and Willbold, D. (2012) Development of a small D-enantiomeric Alzheimer's amyloid-β binding peptide ligand for future *in vivo* imaging applications. *PLoS ONE* **7,** e41457
35. Cohen, S. I., Linse, S., Luheshi, L. M., Hellstrand, E., White, D. A., Rajah, L., Otzen, D. E., Vendruscolo, M., Dobson, C. M., and Knowles, T. P. (2013) Proliferation of amyloid-β42 aggregates occurs through a secondary nucleation mechanism. *Proc. Natl. Acad. Sci. U.S.A.* **110,** 9758–9763
36. Tarawneh, R., and Holtzman, D. M. (2010) Biomarkers in translational research of Alzheimer's disease. *Neuropharmacology* **59,** 310–322
37. Mintun, M. A., Larossa, G. N., Sheline, Y. I., Dence, C. S., Lee, S. Y., Mach, R. H., Klunk, W. E., Mathis, C. A., DeKosky, S. T., and Morris, J. C. (2006) [^{11}C]PIB in a nondemented population: potential antecedent marker of Alzheimer disease. *Neurology* **67,** 446–452
38. Price, J. L., McKeel, D. W., Jr., Buckles, V. D., Roe, C. M., Xiong, C., Grundman, M., Hansen, L. A., Petersen, R. C., Parisi, J. E., Dickson, D. W., Smith, C. D., Davis, D. G., Schmitt, F. A., Markesbery, W. R., Kaye, J., Kurlan, R., Hulette, C., Kurland, B. F., Higdon, R., Kukull, W., and Morris, J. C. (2009) Neuropathology of nondemented aging: presumptive evidence for preclinical Alzheimer disease. *Neurobiol. Aging* **30,** 1026–1036
39. Ladner, R. C., Sato, A. K., Gorzelany, J., and de Souza, M. (2004) Phage display-derived peptides as therapeutic alternatives to antibodies. *Drug Discov. Today* **9,** 525–529
40. Demattos, R. B., Lu, J., Tang, Y., Racke, M. M., Delong, C. A., Tzaferis, J. A., Hole, J. T., Forster, B. M., McDonnell, P. C., Liu, F., Kinley, R. D., Jordan, W. H., and Hutton, M. L. (2012) A plaque-specific antibody clears existing β-amyloid plaques in Alzheimer's disease mice. *Neuron* **76,** 908–920
41. Funamoto, S., Sasaki, T., Ishihara, S., Nobuhara, M., Nakano, M., Watanabe-Takahashi, M., Saito, T., Kakuda, N., Miyasaka, T., Nishikawa, K., Saido, T. C., and Ihara, Y. (2013) Substrate ectodomain is critical for substrate preference and inhibition of γ-secretase. *Nat. Commun.* 4, 2529
42. Austen, B. M., Paleologou, K. E., Ali, S. A., Qureshi, M. M., Allsop, D., and El-Agnaf, O. M. (2008) Designing peptide inhibitors for oligomerization and toxicity of Alzheimer's β-amyloid peptide. *Biochemistry* **47,** 1984–1992
43. Tjernberg, L. O., Näslund, J., Lindqvist, F., Johansson, J., Karlström, A. R., Thyberg, J., Terenius, L., and Nordstedt, C. (1996) Arrest of β-amyloid fibril formation by a pentapeptide ligand. *J. Biol. Chem.* **271,** 8545–8548
44. Amijee, H., Madine, J., Middleton, D. A., and Doig, A. J. (2009) Inhibitors of protein aggregation and toxicity. *Biochem. Soc. Trans.* **37,** 692–696
45. Chacón, M. A., Barría, M. I., Soto, C., and Inestrosa, N. C. (2004) β-Sheet breaker peptide prevents Aβ-induced spatial memory impairments with partial reduction of amyloid deposits. *Mol. Psychiatry* **9,** 953–961

Downloaded from http://www.jbc.org/ at CURTIN UNIV OF TECHNOLOGY (CAUL) on June 12, 2016

46. Granic, I., Masman, M. F., Kees Mulder, C., Nijholt, I. M., Naude, P. J., de Haan, A., Borbély, E., Penke, B., Luiten, P. G., and Eisel, U. L. (2010) LPYFDa neutralizes amyloid-β-induced memory impairment and toxicity. *J. Alzheimers Dis.* **19,** 991–1005
47. Wiesehan, K., Stöhr, J., Nagel-Steger, L., van Groen, T., Riesner, D., and Willbold, D. (2008) Inhibition of cytotoxicity and amyloid fibril formation by a D-amino acid peptide that specifically binds to Alzheimer's disease amyloid peptide. *Protein Eng. Des. Sel.* **21,** 241–246
48. van Groen, T., Wiesehan, K., Funke, S. A., Kadish, I., Nagel-Steger, L., and Willbold, D. (2008) Reduction of Alzheimer's disease amyloid plaque load in transgenic mice by D3, A D-enantiomeric peptide identified by mirror image phage display. *ChemMedChem* **3,** 1848–1852
49. Wiesehan, K., Buder, K., Linke, R. P., Patt, S., Stoldt, M., Unger, E., Schmitt, B., Bucci, E., and Willbold, D. (2003) Selection of D-amino-acid peptides that bind to Alzheimer's disease amyloid peptide Aβ1–42 by mirror image phage display. *Chembiochem* **4,** 748–753
50. Fluharty, B. R., Biasini, E., Stravalaci, M., Sclip, A., Diomede, L., Balducci, C., La Vitola, P., Messa, M., Colombo, L., Forloni, G., Borsello, T., Gobbi, M., and Harris, D. A. (2013) An N-terminal fragment of the prion protein binds to amyloid-β oligomers and inhibits their neurotoxicity *in vivo*. *J. Biol. Chem.* **288,** 7857–7866
51. Chakravarthy, B., Ménard, M., Brown, L., Hewitt, M., Atkinson, T., and Whitfield, J. (2013) A synthetic peptide corresponding to a region of the human pericentriolar material 1 (PCM-1) protein binds β-amyloid (Aβ1–42) oligomers. *J. Neurochem.* **126,** 415–424
52. Sundaram, R. K., Kasinathan, C., Stein, S., and Sundaram, P. (2012) Novel detox gel depot sequesters β-amyloid peptides in a mouse model of Alzheimer's disease. *Int. J. Pept Res. Ther.* **18,** 99–106
53. Jokerst, J. V., Lobovkina, T., Zare, R. N., and Gambhir, S. S. (2011) Nanoparticle PEGylation for imaging and therapy. *Nanomedicine* **6,** 715–728
54. Harris, J. M., and Chess, R. B. (2003) Effect of pegylation on pharmaceuticals. *Nat. Rev. Drug Discov.* **2,** 214–221
55. Sumbria, R. K., Boado, R. J., and Pardridge, W. M. (2012) Imaging amyloid plaque in Alzheimer's disease brain with a biotinylated Aβ peptide radiopharmaceutical conjugated to an IgG-avidin fusion protein. *Bioconjug. Chem.* **23,** 1318–1321
56. Tanifum, E. A., Dasgupta, I., Srivastava, M., Bhavane, R. C., Sun, L., Berridge, J., Pourgarzham, H., Kamath, R., Espinosa, G., Cook, S. C., Eriksen, J. L., and Annapragada, A. (2012) Intravenous delivery of targeted liposomes to amyloid-β pathology in APP/PSEN1 transgenic mice. *PLoS ONE* **7,** e48515
57. Campbell M., Hanrahan, F., Gobbo, O. L., Kelly, M. E., Kiang, A. S., Humphries, M. M., Nguyen, A. T., Ozaki, E., Keaney, J., Blau, C. W., Kerskens, C. M., Cahalan, S. D., Callanan, J. J., Wallace, E., Grant, G. A., Doherty, C.P., and Humphries, P. (2012) Targeted suppression of claudin-5 decreases cerebral oedema and improves cognitive outcome following traumatic brain injury. *Nat. Commun.* **3,** 849
58. Klunk, W. E., Engler, H., Nordberg, A., Wang, Y., Blomqvist, G., Holt, D. P., Bergström, M., Savitcheva, I., Huang, G. F., Estrada, S., Ausén, B., Debnath, M. L., Barletta, J., Price, J. C., Sandell, J., Lopresti, B. J., Wall, A., Koivisto, P., Antoni, G., Mathis, C. A., and Långström, B. (2004) Imaging brain amyloid in Alzheimer's disease with Pittsburgh Compound-B. *Ann. Neurol* **55,** 306–319
59. Okamura, N., and Yanai, K. (2010) Florbetapir (18F), a PET imaging agent that binds to amyloid plaques for the potential detection of Alzheimer's disease. *IDrugs* **13,** 890–899
60. Rinne, J. O., Wong, D. F., Wolk, D. A., Leinonen, V., Arnold, S. E., Buckley, C., Smith, A., McLain, R., Sherwin, P. F., Farrar, G., Kailajärvi, M., and Grachev, I. D. (2012) [^{18}F]Flutemetamol PET imaging and cortical biopsy histopathology for fibrillar amyloid β detection in living subjects with normal pressure hydrocephalus: pooled analysis of four studies. *Acta Neuropathol.* **124,** 833–845
61. Kayed, R., Head, E., Thompson, J. L., McIntire, T. M., Milton, S. C., Cotman, C. W., and Glabe, C. G. (2003) Common structure of soluble amyloid oligomers implies common mechanism of pathogenesis. *Science* **300,** 486–489
62. Lambert, M. P., Velasco, P. T., Chang, L., Viola, K. L., Fernandez, S., Lacor, P. N., Khuon, D., Gong, Y., Bigio, E. H., Shaw, P., De Felice, F. G., Krafft, G. A., and Klein, W. L. (2007) Monoclonal antibodies that target pathological assemblies of Aβ. *J. Neurochem.* **100,** 23–35
63. Mathis, C. A., Wang, Y., and Klunk, W. E. (2004) Imaging β-amyloid plaques and neurofibrillary tangles in the aging human brain. *Curr. Pharm. Des.* **10,** 1469–1492
64. Yates, E. A., Owens, S. L., Lynch, M. F., Cucco, E. M., Umbaugh, C. S., and Legleiter, J. (2013) Specific domains of Aβ facilitate aggregation on and association with lipid bilayers. *J. Mol. Biol.* **425,** 1915–1933

Downloaded from http://www.jbc.org/ at CURTIN UNIV OF TECHNOLOGY (CAUL) on June 12, 2016

Validation and Characterization of a Novel Peptide That Binds Monomeric and Aggregated β-Amyloid and Inhibits the Formation of Neurotoxic Oligomers

Renae K. Barr, Giuseppe Verdile, Linda K. Wijaya, Michael Morici, Kevin Taddei, Veer B. Gupta, Steve Pedrini, Liang Jin, Joseph A. Nicolazzo, Erin Knock, Paul E. Fraser and Ralph N. Martins

J. Biol. Chem. 2016, 291:547-559.
doi: 10.1074/jbc.M115.679993 originally published online November 4, 2015

Access the most updated version of this article at doi: 10.1074/jbc.M115.679993

Alerts:
- When this article is cited
- When a correction for this article is posted

Click here to choose from all of JBC's e-mail alerts

This article cites 64 references, 21 of which can be accessed free at
http://www.jbc.org/content/291/2/547.full.html#ref-list-1

Downloaded from http://www.jbc.org/ at CURTIN UNIV OF TECHNOLOGY (CAUL) on June 12, 2016